Available online at www.sciencedirect.com

SCIENCE DIRECT

Experimental Cell Research 305 (2005) 42–50

Experimental Cell Research

www.elsevier.com/locate/yexcr

Reversible and repeatable linear local cell force response under large stretches

Shengyuan Yang, Taher Saif*

Department of Mechanical and Industrial Engineering, University of Illinois at Urbana-Champaign, 1206 West Green Street, Urbana, IL 61801, USA

Received 25 November 2004, revised version received 16 December 2004

Abstract

Large stretching and un-stretching force response of adherent fibroblasts is measured by micromachined mechanical force sensors. The force sensors are composed of a probe and flexible beams. The probe, functionalized by fibronectin, is used to contact the cells. The flexible beams are the sensing element. The sensors are made of single crystal silicon and fabricated by the SCREAM process. The maximum cell stretch reached is ~50 μm, which is about twice of the cell initial size, and the time delay between two consecutive stretching/un-stretching steps is 75 s unless otherwise stated. We find that the force response of the cells is strongly linear, reversible, and repeatable, with a small stiffening at the initial deformation stage. Force response of single cells measured before and after cytochalasin D treatment suggests that actin filaments take almost all the cell internal forces due to stretch. These findings may shed light on the increasing understanding on the mechanical behavior of cells and provide clues for making new classes of biological materials having uncommon properties.

Keywords: Cell mechanics; Single living cells; Force response; Large deformation; Linear; Reversible and repeatable; Actin filaments; Microelectromechanical systems (MEMS)

Introduction

During the past decade, cell mechanics has received increasing attention due to the influence of intracellular and extracellular forces on cell adhesion, migration, growth, differentiation, apoptosis, gene expression, and signal transduction [1–12]. Significant effort has been directed to the measurement of the force response of single living cells due to deformation. Experimental techniques that are employed include micropipettes [13], optical tweezers [14], magnetic twisting cytometry [1], magnetic bead microrheometry [15], atomic force microscopy (AFM) [16], and surface force apparatus [17]. Such efforts revealed significant insight on the mechanical behavior of cells under small deformations (~1–2 μm or less). There are, however, numerous instances where the cells may be under large deformation. For example, a skeletal muscle can contract to half its optimal length or expand by 50% under physiological conditions. Muscle fibers (cells) in the skeletal muscle may also experience such large deformations [18]. In diffuse axonal injury, the microscopic shear strains could be higher than 50% [19]. The shape of initially rounded rabbit dermal fibroblasts, growing in a collagen–GAG matrix, could be elongated up to an average aspect ratio of 2.8 during the first 15 h in culture [20]. In tensile experimental testing of mechanical properties of soft biological tissues that consists of many cells, stretches more than 50% are normally reached, and some of the cells in the tissues should be subjected to stretches larger than 50% [21,22].

Studies on cell mechanical behavior due to large deformations are limited. The tension and oscillatory stiffness of isolated cardiac myocytes were measured by a pair of micropipettes, and it was found that the cell force response relaxes at each stretch increment [23]. The force versus elongation of single rabbit fibroblasts was measured by a pair of micropipettes, and the force response from six

* Corresponding author. Fax: +1 217 244 6534.
E-mail address: saif@uiuc.edu (T. Saif).

0014-4827/$ - see front matter © 2005 Elsevier Inc. All rights reserved.
doi:10.1016/j.yexcr.2004.12.026

cells was averaged and was found to be linear with deformation [24]. The nonlinear force response due to compression was observed for single bovine endothelial cells by a pair of microplates [25]. Linear force response was observed under stretch for single rat fibroblasts by a functionalized biomicroelectromechanical system (bioMEMS)-based force sensor [26].

Studies on the cell unloading mechanical response are rare, regardless of small or large deformation. AFM was used to load and unload single yeast cells by small indentation, and force response was found to be linear and reversible [27]. A pair of microplates was used to compress and decompress suspended single bovine endothelial cells, and nonlinear reversible force response was reported, but no data were presented [25].

A fundamental question related to the cell force response due to deformation is the mechanism by which the cell resists deformation. It is generally believed that actin filaments of cell cytoskeleton play a key role in taking the cell internal forces [1,26,28–30]. Experiments show that the treatment of a cell with Cyto D (cytochalasin D, a drug that disrupts the actin filaments in a cell) significantly decreases the mechanical response of the cell. For example, Cyto D suppressed the stiffening of the cytoskeleton of endothelial cells [1]. In Ref. [31], two sets of single chick fibroblasts were stretched by a fixed amount of deformation, with one set treated with Cyto D and the other untreated. The average tension in the Cyto D-treated fibroblasts was found to decrease, but it did not vanish even after 50 min. Cyto D-treated connective tissue models also showed reduced force response under stretch [32]. Stiffness decrease due to Cyto D was observed for airway smooth muscle cells, but complete suppression was not observed (more than 25% of the stiffness left after treatment with 10 μM Cyto D compared to that for the untreated cells) [33].

In this paper, we use functionalized bioMEMS-based force sensors to stretch and un-stretch single living cells and measure their force response. The time span of the experiments is slow enough so that the cells can adapt to the applied stretches biologically. Hence, the measured force response is not only mechanical but biological as well. We show that the force response is strongly linear, reversible, and repeatable with no appreciable creep and relaxation. The force response shows small stiffening at the initial deformation stage. The same cells when tested after Cyto D treatment show negligible force response, giving the direct evidence that actin filaments play a key role in taking the cellular internal forces.

Materials and methods

Basic idea

A bioMEMS sensor used here consists of a probe and microflexible beams which act as the cell force sensor (Fig. 1A). The probe and the sensor beams are made of single crystal silicon. The silicon chip (sensor base) is held by a x–y–z piezoelectric actuator. The probe is functionalized by coating with fibronectin (to simulate the cell–extracellular matrix adhesion). It is then brought in contact with a cell for 20 min. The cell forms adhesion sites with the probe most likely by focal adhesion complex activation [34]. The cell can be stretched by moving the sensor base away from the cell using the piezoelectric actuator. The cell applies a force on the probe which is measured from the deflection of the beams and their combined spring constant. Fig. 1B schematically shows a stretched cell. Here the spring represents the beams with a combined spring constant k. In the stretched state, the sensor base is moved by to R to the right by the piezoelectric actuator. The deformation, D, of the cell is given by the movement of the sensor probe. The deflection of the sensing spring is $w = R - D$. Thus the cell force response is $F = kw$. Force response of the cell is given by the measured (F, D) relation. Note that although the spring is linear, (F, D) relation may be nonlinear. For example, if the cell does not provide any restoring force against deformation, then $R = D$ and $F = 0$ for all D.

BioMEMS sensors

Two types of bioMEMS sensors were designed and fabricated. Figs. 1C–E show the type of sensors which can only measure the cell force response in the x direction. Here, two parallel fixed–fixed beams act as the force sensor. They are connected by a backbone structure and hence act as a single spring. A probe is attached to the backbone to contact the cells. The dimension of each beam is length × width (in plane) × depth = 1.96 mm × 0.77 μm × 10.5 μm, the space between the two beams is 300 μm, and the length of the backbone between the right beam and the probe is 1 mm (Fig. 1C). The width and depth of the probe tip that contacts the cells are 2.0 μm and 10.5 μm, respectively (Fig. 1E). Hence, the sensor is compliant in the x direction but stiff in the y and z directions. In cell force response measurements, the sensor moves in the x direction, driven by the piezoelectric actuator. Thus, if the cell force response is not collinear with the direction of stretch, i.e., x direction, the sensor measures only the x component of cell force response. The stiffness of the sensor in the x direction is estimated, from the geometry and elastic modulus of silicon, as 3.4 nN μm^{-1}. From the displacement measurement resolution of 0.14 μm, we have the force resolution of 0.5 nN.

Fig. 1F schematically shows the class of sensors which can measure the cell force response in both the x and y directions. Here, a cantilevered beam acts as the force sensor. A rigid bar is attached to the free end of the beam, and the probe is attached to the free end of the bar. Suppose, the piezoelectric actuator moves the sensor base along the x direction by R_x, and the corresponding cell deformations are D_x and D_y in the x and y directions, respectively. Then the

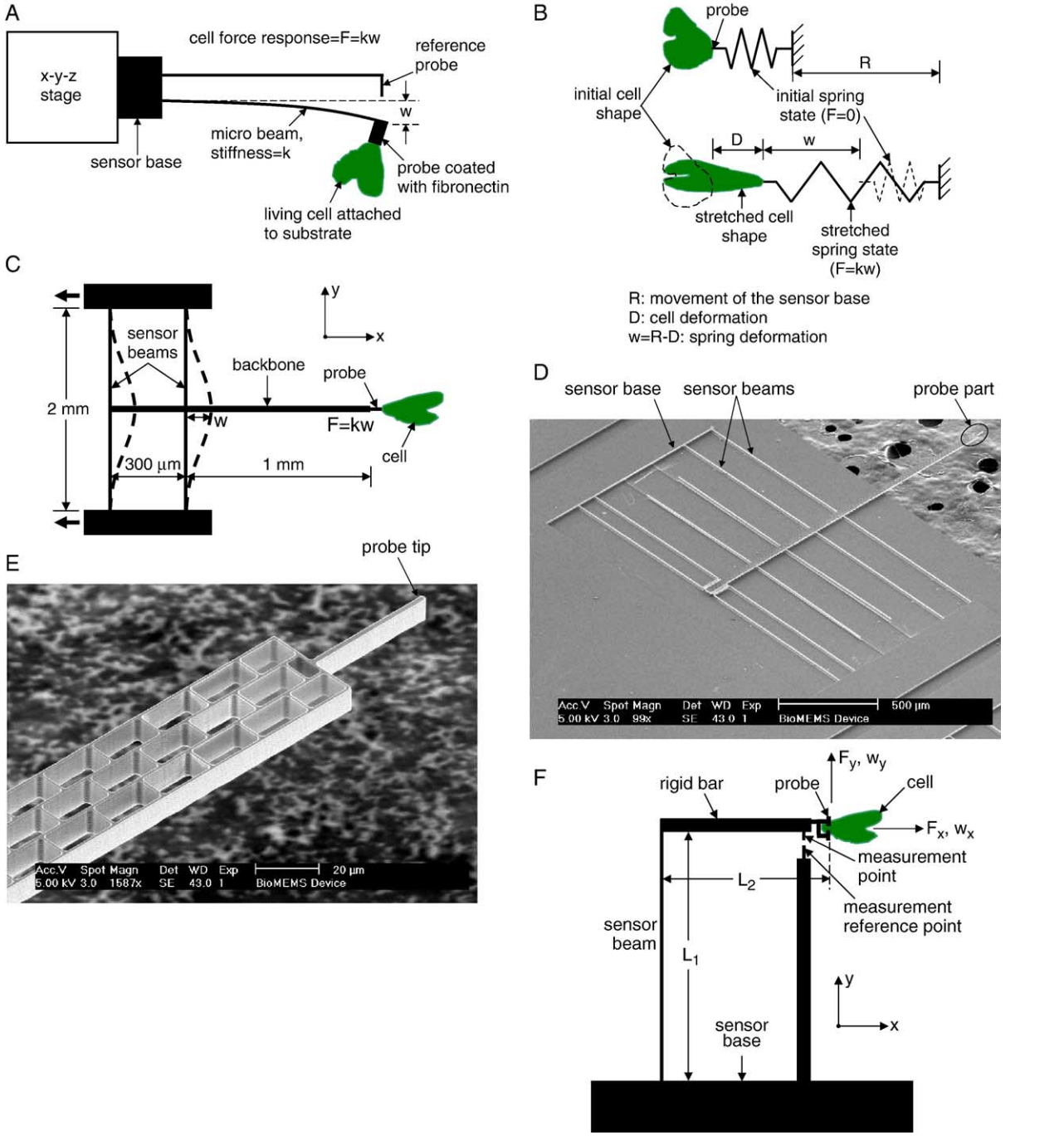

Fig. 1. BioMEMS-based sensors for the study of cell force response. (A) Basic idea of bioMEMS-based method for the study of cell force response. (B) Schematic showing the measurements of cell deformation and deflection of the beams. (C) Schematic of a bioMEMS sensor that can only measure cell force response in the x direction. (D) Scanning electron microscope image of the sensor sketched in C. (E) Probe part of the sensor that contacts the cells. (F) Schematic of a bioMEMS sensor that can measure cell force response in both the x and y directions.

translations (referred to as the sensor deflections in the below) of the probe tip, w_x and w_y, with respect to the sensor base in the x and y directions, respectively, are given by

$$w_x = R_x - D_x$$
$$w_y = D_y. \quad (1)$$

The cell force components, F_x and F_y, in the x and y directions, respectively, relate to w_x and w_x by

$$\begin{bmatrix} F_x \\ F_y \end{bmatrix} = \frac{2EI}{L_1} \begin{bmatrix} \frac{6}{L_1^2} & \frac{3}{L_1 L_2} \\ \frac{3}{L_1 L_2} & \frac{2}{L_2^2} \end{bmatrix} \begin{bmatrix} w_x \\ w_y \end{bmatrix} \quad (2)$$

where E is the Young's modulus of the beam and bar I is the moment of inertia of the cross-section of the beam. The deri-

vation of Eq. (2) is given in Appendix A. Here, the cross-sectional dimensions of the beam are width × depth = 2.0 μm × 13.1 μm, and L_1 = 1 mm, L_2 = 429 μm. The force resolution of the measurement system with this type of sensors is estimated as 0.6 nN.

Sensor fabrication

The MEMS devices were fabricated by the SCREAM process [35]: (1) grow 1 μm thick SiO_2 layer on the surface of the wafer by thermal oxidation; (2) transfer the pattern of the mask for a MEMS sensor to the oxide surface by photolithography; (3) transfer the pattern to silicon by reactive ion etching (RIE); (4) anisotropically etch silicon to the desired depth, about 20 μm, by inductively coupled plasma (ICP); (5) thermally-oxidize the wafer again to put a protecting oxide layer on vertical silicon surface; (6) anisotropically remove the oxide layer on the floor of the patterned trench by RIE; (7) anisotropically etch down the exposed silicon again for an additional depth, about 10 μm, by ICP; (8) isotropically etch the exposed silicon to release the beams, by ICP; (9) remove all the oxide from the device, by wet hydrofluoride acid etching, to get the final sensors made from pure single crystal silicon.

Cell culture and force response measurement

The MEMS sensors were incubated in 50 μg ml^{-1} fibronectin (BD Biosciences) solution at room temperature for 6 h for coating. The cells were cultured from a monkey kidney fibroblast (MKF) cell line, CV-1 (ATCC). The culture medium contains 90% Dulbecco's Modified Eagle's Medium (ATCC) and 10% fetal bovine serum (ATCC), and the cells were incubated in an incubator with 37°C temperature, 5% CO_2 and 98% humidity. The probes of the sensors were brought in contact with the cells for 20 min to form the focal adhesion before the force response measurements started. The force response measurements were conducted at room temperature. An inverted optical microscope (Olympus CK40) with an objective of 10× was used to monitor the deformation of the cell and the displacement of sensor probes. A cooled CCD camera (Olympus MagnaFire S99806) and its data acquisition software were used for imaging and dimensional measurement.

We define the deformation of a cell in the x direction as positive when the cell is elongated, and negative when the cell is indented; the deformation in the y direction is positive upward. The sensor deflection in the x direction is positive when the probe tip moves towards the right for the configuration in Figs. 1C and F; the sensor deflection in the y direction is positive upward. Similarly, the cell force response, acting on the probe, in the x direction is positive when it is towards the right for the configuration in Figs. 1C and F; the cell force response in the y direction is positive upward. Eqs. (1) and (2) complied with these definitions. The cell deformations, sensor deflections, and force response were measured relative to the initial configuration of the cell after contact with the probe unless otherwise stated. During all the measurements, the time delay between two consecutive deformations was kept at 75 s unless otherwise stated.

Results and discussion

Single component force response

Fig. 2 shows the measured force response of an MKF with one stretching and un-stretching cycle. Clearly, the force response is strongly linear and reversible, with a small stiffening at the initial deformation stage. Fig. 3 shows the measured force response of an MKF with more stretching and un-stretching cycles. The contact between the probe tip and the cell was broken at the end of Stretching-3. Here, although there are significant translations between the loading and unloading curves for the first and second cycles (for example, the unloading curve for the first cycle reaches zero force response at a cell deformation of about 15 μm), the general trend of the force response is not only strongly linear and reversible, but also strongly repeatable. Note that the force response curve for Un-stretching-2 is significantly higher than that for Stretching-2, which is not possible for a traditional material since the released elastic energy during unloading should be lower than or equal to that gained during loading. But for living cells, this may not be always the case. During the force response measurement, the cells may response to the external stretching by actively producing contraction [32] and rearrange their internal structures, which may result in higher unloading force response than loading force response. The extra energy

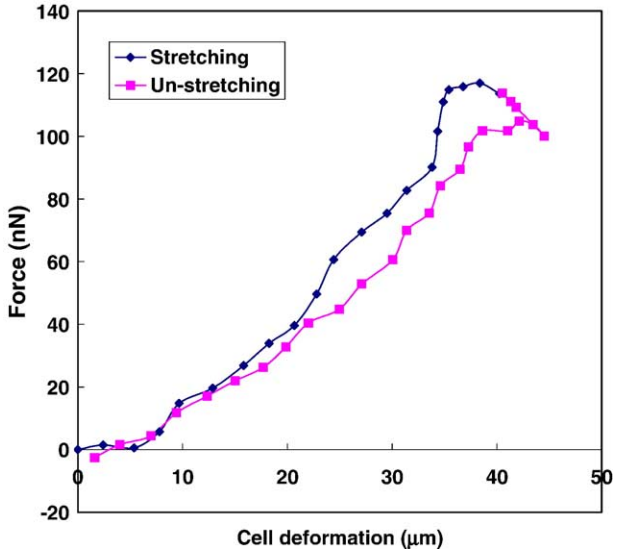

Fig. 2. Measured linear and reversible force response of a monkey kidney fibroblast.

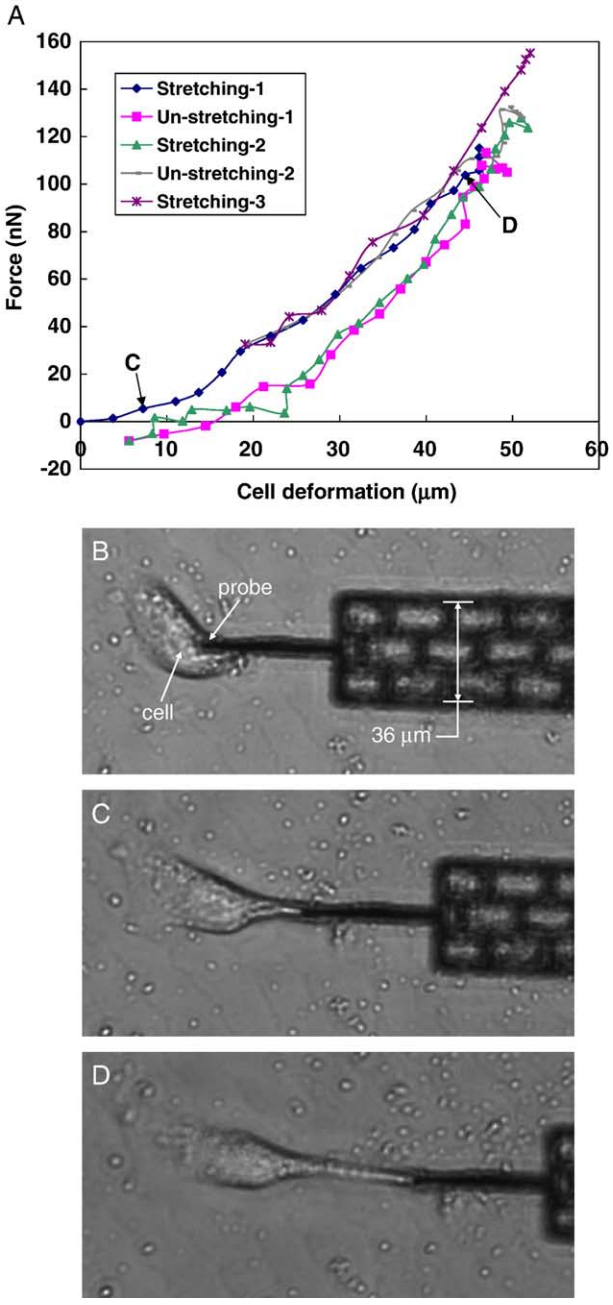

Fig. 3. Measured linear, reversible, and repeatable force response of a monkey kidney fibroblast. (A) Cell force response versus cell deformation. (B–D) Phase images of the MKF right after the probe attachment (no stretch), and at two deformation states corresponding to points C (small stretch) and D (large stretch) in A, respectively.

required for this phenomenon to occur comes from the power plants of the living cells.

The two experiments for Figs. 2 and 3 were done with the sensor shown in Fig. 1C, and the maximum stretching of the cells was about 50 μm, which is approximately twice the cell's initial size (before the stretching experiment). In order to investigate any possible creep/relaxation force response behavior, we varied the time delay between two consecutive force measurements from 1 s to 195 s. We observed a similar cell force response as shown in Fig. 3A, and no appreciable (within the resolution of the measurement system) cell creep/relaxation was observed. Small permanent deformation was always observed for all the loading rates.

Based on current knowledge on the mechanical behavior of living cells [36–38], for example, cytoskeleton stiffens under deformation [28] and the cell is strongly viscoelastic [16], the force response of a living cell due to a large deformation was expected to be nonlinear and irreversible. Our finding contradicts this expectation. Our finding indicates that the cell response to a large deformation may involve reversible biological and biochemical processes with minimal energy loss, which may provide a possible mechanism that nature has adopted to achieve high energy efficiency in living biological systems [39]. This finding may also provide clues for making new classes of biological materials having uncommon properties. For example, directed growth of biological tissues from cells on designed substrates may have the strong linear, reversible, and repeatable force response under large stretches.

Two component force response

The sensor shown in Fig. 1F was used to measure the force response of an MKF. Here, the silicon chip was moved by the piezoelectric actuator in the x direction. Now, the probe tip moves along both the x and y directions, giving cell deformations D_x and D_y. Fig. 4A shows the measured sensor deflections (w_x,w_y), for the cell as it was stretched and un-stretched. We find that the deflection response is strongly reversible and repeatable for the first three stretching and un-stretching cycles (i.e., Stretching-1 and Un-stretching-1, Stretching-2 and Un-stretching-2, and Stretching-3 and Un-stretching-3). The linear trendline for the Stretching-1 gives $w_y = -0.61\ w_x$, which is close to the theoretical relationship $w_y = -0.63\ w_x$ for $F_y = 0$. However, at the last few data points of Un-stretching-1, (w_x,w_y) significantly deviates from $w_y = -0.61\ w_x$, implying F_y. There is also a significant deviation near the end of Un-stretching-2 and the beginning of Stretching-3 from this linear trendline. But, the overall trend of (w_x,w_y) for each of the stretching or un-stretching process in these three cycles shows that the force component in the y direction can be neglected.

Fig. 4B shows the cell deformations, (D_x,D_y), for the cyclic cell stretching and un-stretching experiment. Here, the maximum cell deformation for each cycle decreases for the first three cycles. The cell deformation is strongly reversible for each cycle of these three cycles, which implies that the cell recovers its original state by tracing back its original deformation process. Fig. 4C shows the plot of the cell force response versus the corresponding cell deformation in the x direction. We see strong linear and reversible cell force response for each of the first three cycles of the stretching and un-stretching. We again see that, at some cell deformations, the force response for the unloading processes

is higher than that for the corresponding loading processes of these three cycles. In Figs. 4B and C, the shifts in the cell deformation and force response plots between the first three stretching and un-stretching cycles are due to the produced permanent deformation in the *y* direction. Fig. 4D shows the phase image right before the force response measurement, where the relative displacements between the reference point and the measurement point in the *x* direction indicate the force after initial cell deformation. Figs. 4E–G correspond to the points E–G in Fig. 4C, respectively. Figs. 4D–F show that the cell underwent rotation with respect to a fixed point, thus aligning along the stretch direction.

Effect of Cyto D treatment

In order to explore the role of actin filaments in taking the cell force response, experiments were carried out on MKFs before and after treating them with Cyto D (Sigma, 10 μg ml^{-1}). An initial stretch was applied to each cell and its force response was measured. Cyto D was then applied. For the experiment shown in Fig. 4, the cell changed its shape and relaxed (see Figs. 4G and H) within 3 s after the application of Cyto D. Its shape and force response remain unchanged within the following 5 min, after which the cell was stretched and its force response measured. This observation of fast cell relaxation within few seconds and remaining stable afterwards is in contrast to the results reported in Ref. [40], where it took 20–120 min for Cyto D to take effect. There was also no detachment of the cell from the substrate or the probe during the measurements "After Cyto D". Note the three cycles of stretching and un-stretching measurements (already discussed in the above) conducted before the application of Cyto D are marked by "Before Cyto D" in Fig. 4. The cell deformations, sensor deflections, and force response for "After Cyto D" were measured relative to the initial configuration of the cell when Stretching-4 was started.

In Fig. 4, two cyclic stretching and un-stretching (i.e., Stretching-4 and Un-stretching-4, and Stretching-5 and Un-stretching-5) for "After Cyto D" were done. From Fig. 4A, we see very small sensor deflections for "After Cyto D". From Fig. 4B, we see a significant decrease in the cell deformation in *y* direction for "After Cyto D". The small cell deformation in the *y* direction but large deformation in the *x* direction implies that the cell force acting on the sensor is negligible, i.e., the sensor is moving almost as a rigid body in the *x* direction. From Fig. 4C, by comparing the trends of the cell force response for "Before Cyto D" and "After Cyto D", respectively, we see the cell force response is almost 100% suppressed due to treatment of Cyto D, which shows that the actin filaments are the primary contributors in providing cell force response. The hysteresis in cell force response for the first stretching and un-stretching cycle of "After Cyto D" is much larger than "Before Cyto D".

We also observed significant viscous force response for "After Cyto D". For example, in the first stretching process

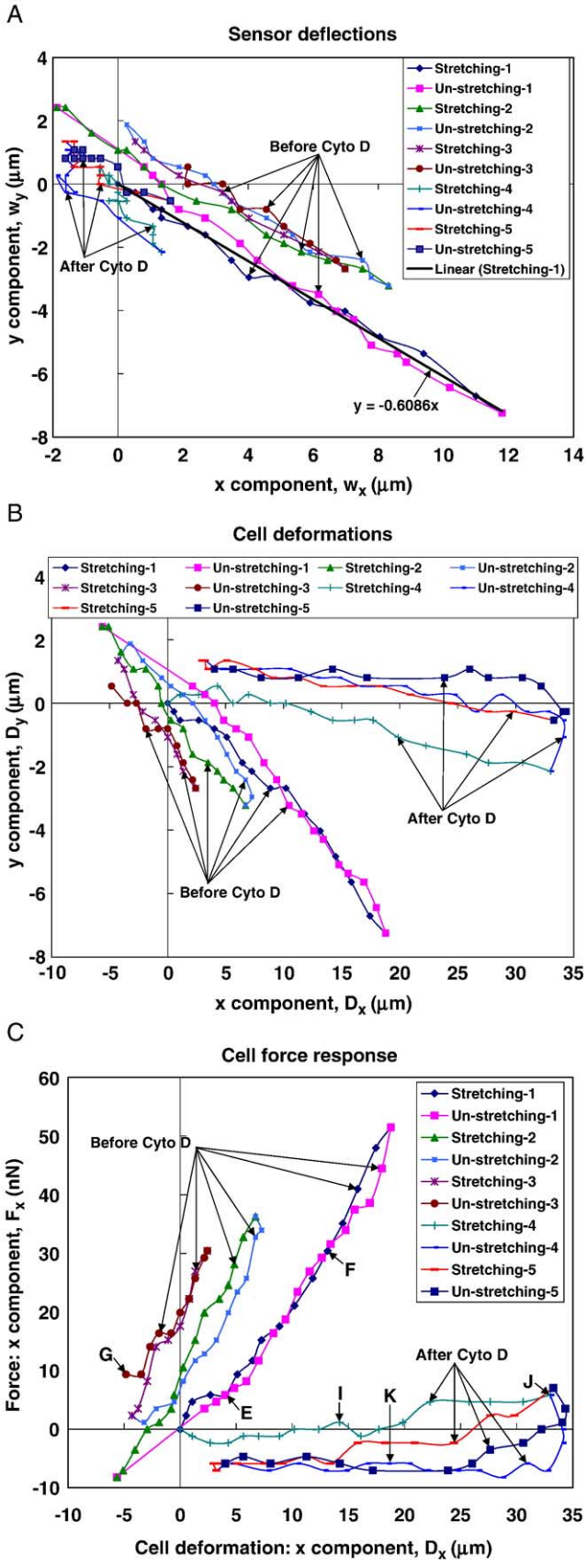

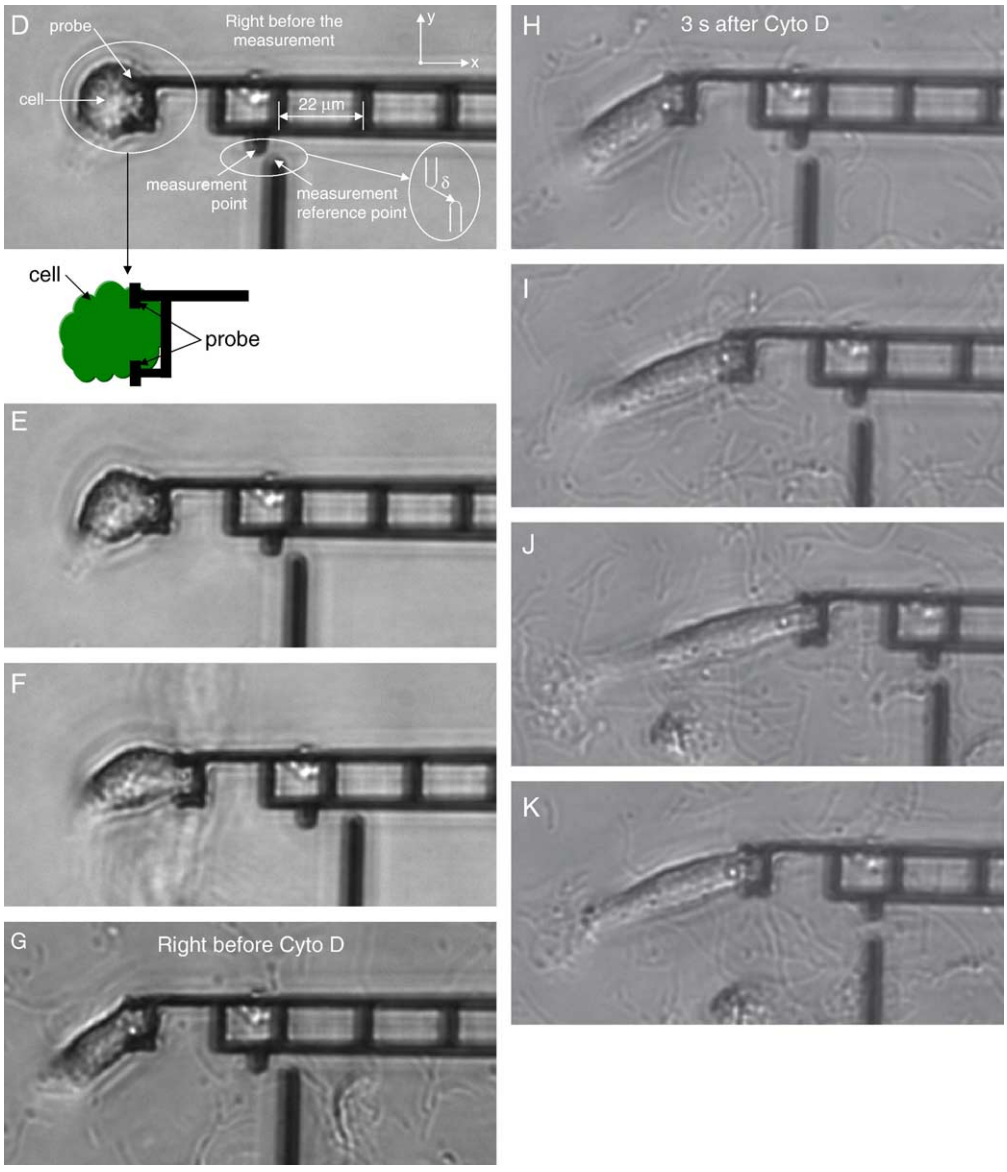

Fig. 4. Cyclic cell stretching and un-stretching force response measurement of a monkey kidney fibroblast by the force sensor shown in Fig. 1F and the effect due to Cyto D treatment. (A) Sensor deflections in the x and y directions. (B) Cell deformations in the x and y directions. (C) Cell force response versus the cell deformation in the x direction. (D) Phase image right before the force response measurement. (E–G) Correspond to the phase images for the points E–G for "Before Cyto D" in C, respectively, and G is also the phase image right before the addition of Cyto D. (H) Phase image 3 s after the addition of Cyto D. (I–K) Correspond to the phase images for the points I to K for "After Cyto D" in C, respectively.

for "After Cyto D", we fixed the sensor base at cell deformations of 33.0 μm and 2.1 μm (in the x and y directions, respectively). We found, after 1 min, the cell deformations changed to 34.1 μm and 1.1 μm, while the x component cell force relaxed from 5.8 nN to 0 (note that the x component of the absolute cell force response is still not 0 since the cell force response data are measured relative to the initial configuration of the cell after contact with the probe, where the probe is subjected to a small force). In the second stretching process for "After Cyto D", similarly, we fixed the sensor base at cell deformations of 33.3 μm and 0.5 μm in the x and y directions, respectively. After 1 min, the corresponding cell deformations changed to 34.3 μm and 0.3 μm, while the x component cell force relaxed from 7.0 nN to 3.5 nN. Note that we did not observe any appreciable relaxation for "Before Cyto D", which suggests that the viscosity of the cell for "After Cyto D" might be much larger than that for "Before Cyto D". The enhanced viscosity for "After Cyto D" is possibly due to depolymerization of actin filaments (which may increase the viscosity of the cytoplasm). However, in Fig. 4B, for "After Cyto D", the cell recovers its original state by following the deformation history of the stretching process except the small plastic deformation, which indicates the role of the elastic cell membrane in the recovery process.

Figs. 4G and H show the cell right before the application of Cyto D (i.e., the end point of Un-stretching-3) and 3 s after. The latter shows the decrease of cell force response (compare the sensor deflection). Figs. 4I–K correspond to images for the points I–K for "After Cyto D" in Fig. 4C, respectively. The cell shape and deformation recovery for the un-stretching process is reflected in these figures. Figs. 4H and I show that the cell continued to relax during the initial stretching stage for "After Cyto D".

Conclusions

We have demonstrated that functionalized bioMEMS can be applied as a simple basic tool for manipulating living cells and measuring their force response. The cell force response has been shown to be strongly linear, reversible, and repeatable subject to large stretches. Cells aligned with the stretch direction, which makes the transverse force response negligible. Actin filaments have been shown to play a dominant role in taking the cell internal force. Without actin filaments, cell force response is relatively negligible.

Acknowledgments

We thank Prof. N. Wang of Harvard School of Public Health and Prof. V. I. Gelfand of the Department of Cell and Structural Biology at the University of Illinois at Urbana-Champaign for helpful discussion on this work. This work was supported by NSF (ECS 01-18003).

Appendix A

For the sensor shown in Fig. 1F, the displacements of the probe tip in the x and y directions are induced by either F_x or F_y or both. For example, F_x deforms the sensor beam in the x direction and rotates its free end. This rotation tilts the rigid bar, which moves the probe tip in the y direction. Similarly, F_y also induces sensor deflections in both x and y directions. In Fig. 4A, the absolute maximum sensor deflection in the x direction is 11.8 μm, which is only 1.18% of the length of the sensor beam (L_1 = 1 mm). The absolute maximum sensor deflection in the y direction is 7.2 μm, which is only 1.68% of the length of the rigid bar (L_2 = 429 μm). Thus, we assume that the beam is subjected to small deformation and rotation in finding the analytical expressions for the sensor deflections.

The deflection in the x direction and rotation (positive counterclockwise) at the free end of the beam induced by F_x alone are given by $F_xL_1^3/3EI$ and $-F_xL_1^2/2EI$, respectively, and such a rotation induces a sensor deflection of $(-F_xL_1^2/2EI)L_2$ in the y direction. F_y creates a bending moment F_yL_2 at the free end of the beam, which in turn alone induces a deflection in the x direction and rotation at the free end of the beam of $-F_yL_2L_1^2/2EI$ and $F_yL_2L_1/EI$, respectively, and such a rotation induces a sensor deflection of $(F_yL_2L_1/EI)L_2$ in the y direction.

According to the linear superimposition, the total sensor deflections induced by F_x and F_y combined are given by

$$w_x = \frac{F_xL_1^3}{3EI} - \frac{F_yL_1^2L_2}{2EI} \text{ and } w_y = -\frac{F_xL_1^2L_2}{2EI} + \frac{F_yL_1L_2^2}{EI} \tag{A1}$$

for the x and y directions, respectively. By inverting Eq. (A1), Eq. (2) is obtained, which is

$$\begin{bmatrix} F_x \\ F_y \end{bmatrix} = \frac{2EI}{L_1} \begin{bmatrix} \frac{6}{L_1^2} & \frac{3}{L_1L_2} \\ \frac{3}{L_1L_2} & \frac{2}{L_2^2} \end{bmatrix} \begin{bmatrix} w_x \\ w_y \end{bmatrix}. \tag{A2}$$

References

[1] N. Wang, J.P. Butler, D.E. Ingber, Mechanotransduction across the cell surface and through the cytoskeleton, Science 260 (1993) 1124–1127.
[2] I.S. Sukharev, B. Martinac, V.Y. Arshavsky, C. Kung, Two types of mechanosensitive channels in the *Escherichia coli* cell envelope: solubilization and functional reconstitution, Biophys. J. 65 (1993) 177–183.
[3] D.C. Van-Essen, A tension-based theory of morphogenesis and compact wiring in the central nervous system, Nature 385 (1997) 313–318.
[4] C.S. Chen, M. Mrksich, S. Huang, G.M. Whitesides, D.E. Ingber, Geometric control of cell life and death, Science 276 (1997) 1425–1428.
[5] M.E. Chicurel, C.S. Chen, D.E. Ingber, Cellular control lies in the balance of forces, Curr. Opin. Cell Biol. 10 (1998) 232–239.
[6] K.-D. Chen, et al., Mechanotransduction in response to shear stress, J. Biol. Chem. 274 (1999) 18393–18400.
[7] E.C. Breen, Mechanical strain increase type I collagen expression in pulmonary fibroblasts in vitro, J. Appl. Physiol. 88 (2000) 203–209.
[8] M. Salvador-Silva, C.S. Ricard, O.A. Agapova, P. Yang, M.R. Hernandez, Expression of small heat shock proteins and intermediate filaments in the human optic nerve head astrocytes exposed to elevated hydrostatic pressure in vitro, J. Neurosci. Res. 66 (2001) 59–73.
[9] Y. Sawada, M.P. Sheetz, Force transduction by triton cytoskeletons, J. Cell Biol. 156 (2002) 609–615.
[10] D.J. Webb, J.T. Parsons, A.F. Horwitz, Adhesion assembly, disassembly and turnover in migrating cells-over and over and over again, Nat. Cell Biol. 4 (2002) E97–E100.
[11] C.H. Thomas, J.H. Collier, C.S. Sfeir, K.E. Healy, Engineering gene expression and protein synthesis by modulation of nuclear shape, Proc. Natl. Acad. Sci. U. S. A. 99 (2002) 1972–1977.
[12] P.F. Davies, J. Zilberberg, B.P. Helmke, Spatial microstimuli in endothelial mechanosignaling, Circ. Res. 92 (2003) 359–370.
[13] E. Evans, D. Berk, A. Leung, Detachment of agglutinin-bonded red-blood-cells: 1. Forces to rupture molecular-point attachments, Biophys. J. 59 (1991) 838–848.
[14] J. Sleep, D. Wilson, R. Simmons, W. Gratzer, Elasticity of the red cell membrane and its relation to hemolytic disorders: an optical tweezers study, Biophys. J. 77 (1999) 3085–3095.
[15] A.R. Bausch, F. Ziemann, A.A. Boulbitch, K. Jacobson, E. Sackmann, Local measurements of viscoelastic parameters of adherent cell surfaces by magnetic bead microrheometry, Biophys. J. 75 (1998) 2038–2049.

[16] J. Alcaraz, et al., Microrheology of human lung epithelial cells measured by atomic force microscopy, Biophys. J. 84 (2003) 2071–2079.
[17] C.A. Helm, W. Knoll, J.N. Israelachvili, Measurement of ligand–receptor interactions, Proc. Natl. Acad. Sci. U. S. A. 88 (1991) 8169–8173.
[18] W. Maurel, Y. Wu, N. Magnenat Thalmann, D. Thalmann, Biomechanical Models for Soft Tissue Simulation, Springer-Verlag, Berlin, 1998.
[19] B.J. Pfister, T.P. Weihs, M. Betenbaugh, G. Bao, An in vitro uniaxial stretch model for axonal injury, Ann. Biomed. Eng. 31 (2003) 589–598.
[20] T.M. Freyman, I.V. Yannas, Y.-S. Pek, R. Yokoo, L.J. Gibson, Micromechanics of fibroblast contraction of a collagen–GAG matrix, Exp. Cell Res. 269 (2001) 140–153.
[21] M. Nordin, T. Lorenz, M. Campello, Biomechanics of tendons and ligaments, in: M. Nordin, V.K. Frankel (Eds.), Basic Biomechanics of the Musculoskeletal System, Lippincott Williams and Wilkins, Philadelphia, 2001, pp. 102–125.
[22] K. Hayashi, Mechanical properties of soft tissues and arterial walls, in: G.A. Holzapfel, R.W. Ogden (Eds.), Biomechanics of Soft Tissue in Cardiovascular Systems, Springer Wien, New York, 2003, pp. 15–64.
[23] R.E. Palmer, A.J. Brady, K.P. Roos, Mechanical measurements from isolated cardiac myocytes using a pipette attachment system, Am. J. Physiol. 270 (1996) C697–C704.
[24] H. Miyazaki, Y. Hasegawa, K. Hayashi, A newly designed tensile tester for cells and its application to fibroblasts, J. Biomech. 33 (2000) 97–104.
[25] N. Caille, O. Thoumine, Y. Tardy, J.-J. Meister, Contribution of the nucleus to the mechanical properties of endothelial cells, J. Biomech. 35 (2002) 177–187.
[26] M.T.A. Saif, C.R. Sager, S. Coyer, Functionalized biomicroelectromechanical systems sensors for force response study at local adhesion sites of single living cells on substrates, Ann. Biomed. Eng. 31 (2003) 950–961.
[27] A. Touhami, B. Nysten, Y.F. Dufrene, Nanoscale mapping of the elasticity of microbial cells by atomic force microscopy, Langmuir 19 (2003) 4539–4543.
[28] D. Stamenovic, N. Wang, Cellular responses to mechanical stress, invited review: engineering approaches to cytoskeletal mechanics, J. Appl. Physiol. 89 (2000) 2085–2090.
[29] D.E. Ingber, Tensegrity I. Cell structure and hierarchical systems biology, J. Cell Sci. 116 (2003) 1157–1173.
[30] K. Yu. Volokh, Cytoskeletal architecture and mechanical behavior of living cells, Biorheology 40 (2003) 213–220.
[31] O. Thoumine, A. Ott, Time scale dependent viscoelastic and contractile regimes in fibroblasts probed by microplate manipulation, J. Cell Sci. 110 (1997) 2109–2116.
[32] T. Wakatsuki, M.S. Kolodney, G.I. Zahalak, E.L. Elson, Cell mechanics studied by a reconstituted model tissue, Biophys. J. 79 (2000) 2353–2368.
[33] S.S. An, R.E. Laudadio, J. Lai, R.A. Rogers, J.J. Fredberg, Stiffness changes in cultured airway smooth muscle cells, Am. J. Physiol. 283 (2002) C792–C801.
[34] B. Alberts, A. Johnson, J. Lewis, M. Raff, K. Roberts, P. Walter, Molecular Biology of the Cell, Garland Science, New York, 2002.
[35] K.A. Shaw, Z.L. Zhang, N.C. MacDonald, SCREAM-I: a single mask, single crystal silicon, reactive etching process for microelectromechanical structures, Sens. Actuators, A 40 (1994) 63–70.
[36] C. Zhu, G. Bao, N. Wang, Cell mechanics: mechanical response, cell adhesion, and molecular deformation, Annu. Rev. Biomed. Eng. 2 (2000) 189–226.
[37] G. Bao, S. Suresh, Cell and molecular mechanics of biological materials, Nat. Mater. 2 (2003) 715–725.
[38] J.D. Humphrey, Continuum Biomechanics of soft biological tissues, Proc. R. Soc. Lond., A 459 (2003) 3–46.
[39] H.J. Morowitz, Foundations of Bioenergetics, Academic Press, New York, 1978.
[40] C. Rotsch, M. Radmacher, Drug-induced changes of cytoskeletal structure and mechanics in fibroblasts: an atomic force microscopy study, Biophys. J. 78 (2000) 520–535.